

LETTER • OPEN ACCESS

Linkages between GRACE water storage, hydrologic extremes, and climate teleconnections in major African aquifers

To cite this article: Bridget R Scanlon *et al* 2022 *Environ. Res. Lett.* **17** 014046

View the [article online](#) for updates and enhancements.

You may also like

- [Analysis of the Linkage between South African's Exchange Rate and Stock Price Index](#)
Hsin-Pei Hsueh, Fangjhy Li and Changqing Liu
- [What if there were no food aid and food import: food insufficiency in Africa from the perspective of self-sufficiency](#)
Yanjuan Wu, Rui Chen, Zhiming Feng et al.
- [Global warming threatens agricultural productivity in Africa and South Asia](#)
Benjamin Sultan

ENVIRONMENTAL RESEARCH
LETTERS

LETTER

Linkages between GRACE water storage, hydrologic extremes, and climate teleconnections in major African aquifers

OPEN ACCESS

RECEIVED
28 August 2021REVISED
13 October 2021ACCEPTED FOR PUBLICATION
22 November 2021PUBLISHED
7 January 2022

Original content from
this work may be used
under the terms of the
[Creative Commons
Attribution 4.0 licence](#).

Any further distribution
of this work must
maintain attribution to
the author(s) and the title
of the work, journal
citation and DOI.



Bridget R Scanlon^{1,*} , Ashraf Rateb¹ , Assaf Anyamba², Seifu Kebede³, Alan M MacDonald⁴ ,
Mohammad Shamsudduha⁵ , Jennifer Small², Alexander Sun¹ , Richard G Taylor³ and Hua Xie⁶

¹ Bureau of Economic Geology, Jackson School of Geosciences, University of Texas at Austin, Austin, TX, United States of America

² NASA/Goddard Space Flight Center, Greenbelt, MD, United States of America

³ School of Engineering, Centre for Water Resources Research, University of KwaZulu-Natal (UKZN), Pietermaritzburg, South Africa

⁴ British Geological Survey, Lyell Centre, Edinburgh, United Kingdom

⁵ Department of Geography, University College London, London, United Kingdom

⁶ Environment and Production Technology Division, International Food Policy Research Institute, Washington, DC, United States of America

* Author to whom any correspondence should be addressed.

E-mail: bridget.scanlon@beg.utexas.edu

Keywords: Africa water storage, GRACE satellites, climate teleconnections, sustainable groundwater management, floods and droughts, managed aquifer recharge

Supplementary material for this article is available [online](#)

Abstract

Water resources management is a critical issue in Africa where many regions are subjected to sequential droughts and floods. The objective of our work was to assess spatiotemporal variability in water storage and related controls (climate, human intervention) in major African aquifers and consider approaches toward more sustainable development. Different approaches were used to track water storage, including GRACE/GRACE Follow On satellites for Total Water Storage (TWS); satellite altimetry for reservoir storage, MODIS satellites for vegetation indices, and limited ground-based monitoring. Results show that declining trends in TWS (60–73 km³ over the 18 yr GRACE record) were restricted to aquifers in northern Africa, controlled primarily by irrigation water use in the Nubian and NW Saharan aquifers. Rising TWS trends were found in aquifers in western Africa (23–49 km³), attributed to increased recharge from land use change and cropland expansion. Interannual variability dominated TWS variability in eastern and southern Africa, controlled primarily by climate extremes. Climate teleconnections, particularly El Niño Southern Oscillation and Indian Ocean Dipole, strongly controlled droughts and floods in eastern and southern Africa. Huge aquifer storage in northern Africa suggests that the recent decadal storage declines should not impact the regional aquifers but may affect local conditions. Increasing groundwater levels in western Africa will need to be managed because of locally rising groundwater flooding. More climate resilient water management can be accomplished in eastern and southern Africa by storing water from wet to dry climate cycles. Accessing the natural water storage provided by aquifers in Africa is the obvious way to manage the variability between droughts and floods.

1. Introduction

The United Nations Sustainable Development Goal (SDG) related to water (SDG-6) was established to ensure available and sustainable management of water and sanitation by 2030. An estimated 785 million people globally lacked access to basic water services in 2017, 40% in sub-Saharan Africa (SSA) [1]. Previous studies of groundwater (GW)

resources in Africa suggest large storage volumes (~0.66 million km²), ~100 times greater than annual renewable freshwater resources [2], indicating that these large volumes could provide a buffer against climate change impacts on water resources [3]. While many global studies emphasize GW overexploitation and scarcity, some suggest that GW is underutilized in SSA and could be expanded to support water security, agricultural production, and economic development

[4]. However, other factors may constrain GW development, such as energy access, drilling technologies, and financing. Energy access is increasing through expansion of solar photovoltaic systems in Africa [5]; however, removing fuel-cost constraints could lead to unsustainable GW development [6].

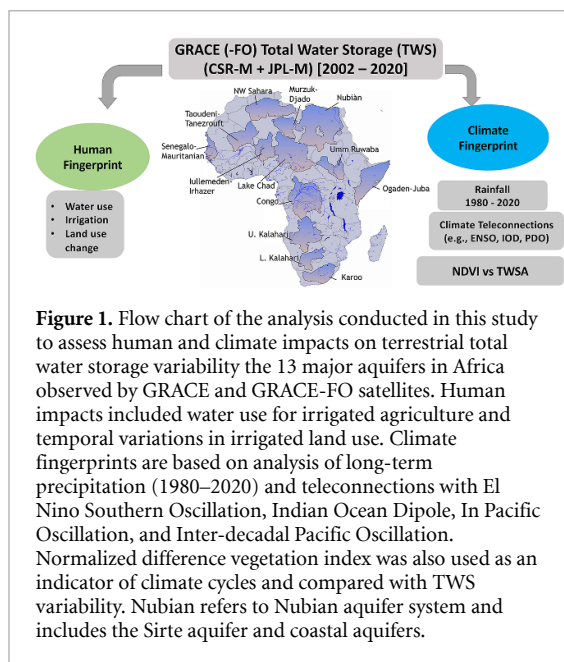
Understanding the dynamics of water resources within the context of climate extremes/change is a prerequisite to expanding GW development in Africa. Limited availability of ground-based monitoring of water resources, particularly in Africa, has resulted in heavy reliance on remote sensing. Many studies have used Gravity Recovery and Climate Experiment (GRACE) satellite data to assess spatiotemporal variability in water storage since 2002. Early studies were based on limited GRACE records [7, 8]; however, recent studies have the advantage of longer records [9, 10]. Several studies noted declining trends in northern African aquifers, with depletion totaling 30–160 km³ over different areas and time periods [9, 11]. Global analyses of GRACE Total Water Storage (TWS: surface water, soil moisture, plus GW) data show increasing trends in many African regions outside of northern Africa, with magnitudes up to ~400 km³ (2003–2016) in the Okavango/Zambesi region; however, many of these apparent trends are attributed to natural climate variability and are not expected to persist over the long term [9]. Another GRACE global study focused on GW storage (GWS) after subtracting surface water storage (SWS) and soil moisture storage (SMS) and emphasizes the nonlinearity in GWS time series, including all aquifers in Africa, attributing the nonlinearity to episodic recharge in these systems [12]. In another global study, the severity of GRACE TWS trends was evaluated relative to multidecadal interannual variability in reconstructed TWS (1979–2019) [13]. GRACE TWS trends exceeding ± 3 standard deviations (SD) in long-term interannual variability were considered exceptional and were recorded in the Niger, Volta, and Okavango river basins [13]. Some studies focused specifically on Africa, combining GRACE data with output from land surface models. One such study noted no substantial declining trends in GWS in any African aquifer but recorded rising trends in western Africa, consistent with rising trends from ground-based monitoring (Senegal and Iullemeden aquifers) [10, 14]. Some studies have focused on the use of *in situ* data to assess GW links to climate using long-term hydrographs and stable isotopes to demonstrate the importance of heavy rainfall events, and ground estimates of decadal GW recharge to map water security [15–17].

Many studies have attempted to assess the causes of TWS variability in Africa, focusing primarily on human intervention and climate. Trends in TWS and GWS in northern Africa have been attributed to GW extraction, primarily for irrigation [9] and natural

long term decline from previous pluvial periods [18]; however, stabilization of TWS variability after 2014 in the Nubian aquifer may be linked to reduced irrigation [11]. Trends in GWS in western Africa, particularly in the Iullemeden aquifer, have been linked to land use changes from deep rooted native vegetation to shallow rooted crops and related increased recharge [14]. Another study linked GRACE-derived GWS rise in the Niger Basin to land use change [19]. Human footprints can also result from dam construction and reservoir installation. Previous studies attributed much of the large decline in storage (83 km²) between 2003 and 2006 in the Lake Victoria Basin tracked by GRACE satellites to human intervention through dam management rather than climate or GW abstraction [20, 21]. Outside of northern Africa, GW development has been limited, indicating that storage changes should be dominated by natural climatic variability [10, 22].

Understanding linkages between climate variability, particularly droughts and floods, and water storage is critical for resource management. Many studies have evaluated the importance of climate teleconnections driving droughts and floods in various regions in Africa. A comprehensive assessment of climate teleconnections on rainfall over the past century emphasizes wet and dry climate cycles in different regions, particularly El Nino Southern Oscillation (ENSO) dipole across eastern and southern Africa [23]. A recent review of the Famine Early Warning System Network emphasizes the interactions between ENSO and subtropical Indian Ocean Dipole (IOD) [24]. Many studies highlight the complexity of rainfall in eastern Africa with teleconnections to ENSO and the IOD, particularly during the short rains in Oct/Nov [25]. Various teleconnections are shown to be associated with GRACE TWS variability in different regions of Africa: North Atlantic Oscillation (NAO) and decreasing TWS in southern Africa, IOD and increasing TWS in equatorial East Africa [26]; ENSO impacts in eastern and southern Africa [22]; ENSO and IOD in the Nile Basin [27–29], and ENSO, Pacific Decadal Oscillation (PDO), NAO, and Atlantic Multidecadal Oscillation (AMO) in Lake Volta [30, 31]. Additional data have been used to support the impact of climate variability, including NDVI emphasizing the ENSO dipole between eastern and southern Africa [32, 33] and altimetry in lakes and reservoirs [34, 35].

Varying water storage dynamics throughout Africa require different management strategies to optimize water resources. Analysis of teleconnections linked to GRACE derived GWS emphasizes the importance of integrated water management to even out water supply variability from wet to dry climate cycles [36]. The objective of our work was to address the following questions:



- What is the spatiotemporal variability in GRACE-derived TWS changes in Africa over 2002–2020?
- How are climate indices linked to GRACE TWS variability through various teleconnections?
- How can we use the results from GRACE satellite data to better manage water resources within the context of climate extremes?

The study is based on GRACE/GRACE-Follow On [GRACE-FO] monthly TWS variability for 13 major aquifers throughout Africa (figure 1). Novel aspects of the study include extension of GRACE data to 2020, application of multiple metrics to assess reliability of long-term linear trends in TWS, evaluating linkages between TWS variability and climate teleconnections using cyclostationary empirical orthogonal function (CSEOF) which does not assume stationarity of the derived temporal components), use of reconstructed GRACE data back to 1960 [37] to evaluate TWS variability derived from longer-term climate cycles, inclusion of additional data to assess hydroclimatic impacts on TWS variability (global models, altimetry reservoir water levels, normalized difference vegetation index (NDVI), and modeled soil moisture); and discussing implications of climate extremes for water management in different regions, particularly eastern and southern Africa.

2. Materials and methods

2.1. GRACE and GRACE-FO data

Monthly GRACE TWS data used in this study include NASA Jet Propulsion Lab. (JPL) [38] and Univ. of Texas Center for Space Research (CSR) [39] mascons solutions (tables S2 and S3, supporting information, section 1.1). Uncertainties in GRACE TWS

anomalies (TWSAs) are based on the standard deviation of GRACE mascon solutions (JPL and CSR) and spherical harmonic solutions (CSR, JPL, and GeoForschungsZentrum (GFZ)) (table S7). GRACE TWS time series was decomposed with Seasonal Trend Decomposition using Loess (STL) [40] (table S8):

$$S_{\text{Raw}} = S_{\text{long term}} + S_{\text{Annual}} + S_{\text{Semi annual}} + S_{\text{residual}}$$

where S is TWS signal; Raw refers to the raw data; and long-term variability includes linear and interannual variability (table S1(a)). A linear trend was applied to long-term variability and the remaining signal is interannual variability (table 1). Trends have been termed ‘apparent trends’ similar to previous studies [9]. Trend reliability or persistence was assessed using three metrics:

- Percentage of total TWS variance explained by linear trends (table S1(a)),
- Goodness of fit of linear trends to TWS variability (R^2 value), and
- Ratio of Trend to Interannual Variability (TIVR), with higher values of each metric suggesting more reliable and persistent trends (table S1).

TIVR was calculated from the ratio of the linear TWS trend to the standard deviation (SD) of interannual variability, similar to previous studies [13, 41]. However, in this study, we used interannual variability from the GRACE data for the period of record (2002–2020) rather than the long-term reconstructed TWS data [37] because the reconstructed TWS data for Africa greatly underestimate interannual TWS variability relative to hydrological modeling output. However, the reconstructed TWS variability still provides information on decadal variability in climate-driven TWS because climate forcing (temperature and precipitation) was used to reconstruct TWS data (table S13).

2.2. Climate variability and controls on TWS variability

The relationship between TWS variability and precipitation time series for the aquifers was evaluated using cross correlations. The monthly precipitation anomaly is based on Integrated Multi-satellitE Retrievals for GPM (Global Precipitation Measurement) (IMERG) data by subtracting the long-term mean (2000–2020) (table S16). The cumulative precipitation anomaly (CPA) was calculated by accumulating the residual after subtracting the climatology (SI, section 2.6; table S17).

Because of the potential importance of floods and droughts on water storage, we evaluated climate teleconnection controls on floods and droughts and linkages to TWS variability (SI, section 1.4). The climate teleconnections represent the natural variability in the Pacific, Indian, and Atlantic oceans, Mediterranean Sea, and Arctic (table S23). Our analysis focused on relatively short-term indices (e.g.

Table 1. Summary of TWSA analysis for the major aquifers in Africa; TWSA trend in mm yr⁻¹ and km³ over 18.3 yrs, coefficient of determination (R²) of the linear trend model for TWSA, standard deviation (SD) of interannual variability from GRACE ensemble mascons (CSR and JPL) for the period 2002–2020, TWS trend over 18.3 years relative to interannual variability (Trend to Interannual Variability, TIVR); Correlation between (TWSA, GWSA), (TWSA, P), and (TWSA NDVI). Net Abs.GW is net abstraction of groundwater rate based on the WGHM model. Detailed information is provided in table S1.

ID	Aquifers Name	TWSA linear trend		R ²	SD Interann.		TIVR	TWSA vs		TWSA vs P	TWSA vs NDVI	Net Abs. GW (km ³ yr ⁻¹)
		mm yr ⁻¹	km ³ /18.3 yr		Variab. (mm)	GWSA		R				
1	Nubian Aquifer	-1.8 ± 0.05	-72.7	0.77	5.0	-84.0	1.00	0.25 (14)	0.09 (7)	2.74		
2	NW Sahara	-3.2 ± 0.21	-60.0	0.88	6.2	-9.6	0.99	0.33 (3)	0.58 (-1)	1.74		
3	Murzuk-Djado	-2.3 ± 0.13	-20.6	0.93	3.1	-13.7	1.00	0.15 (7)	0.19 (-2)	0.52		
4	Senegalo	4.3 ± 0.11	23.0	0.79	12.4	6.3	0.99	0.80 (1)	0.91 (1)	0.13		
5	Taoudeni	-0.2 ± 0.1	-2.9	0.02	5.1	-0.8	0.91	0.24 (1)	0.22 (4)	0.00		
6	Iullemeden	4.6 ± 0.36	49.1	0.87	8.8	9.6	0.99	0.70 (1)	0.83 (0)	0.09		
7	Lake Chad	1.5 ± 0.14	40.6	0.32	13.8	1.9	0.98	0.82 (2)	0.92 (1)	0.13		
8	Umm Ruwaba	-0.2 ± 0.39	-1.9	0.01	20.9	-0.2	0.93	0.87 (3)	0.92 (1)	0.00		
9	Ogaden-Juba	1.7 ± 0.03	34.9	0.38	14.4	2.2	0.69	0.57 (1)	0.74 (0)	0.04		
10	Congo	1.9 ± 0.11	54.1	0.08	31.3	1.2	0.78	0.71 (2)	0.58 (1)	0.12		
11	Upper Kalahari	7.2 ± .33	131.3	0.15	88.3	1.5	0.99	0.73 (2)	0.79 (1)	0.03		
12	Lower Kalahari	0.90 ± 0.03	6.9	0.08	16.5	1.0	0.56	0.56 (2)	0.71 (0)	0.02		
13	Karoo	0.2 ± 0.16	2.1	0.01	17.0	0.2	0.58	0.28 (2)	0.33 (1)	0.14		

ENSO, IOD) because the GRACE record is only 18 yrs. However, we examined some longer-term climate cycles (e.g. AMO and PDO) using climate-driven reconstructed GRACE TWS variability from 1960 to 2014 (table S13) [37]. To obtain consistent physical patterns of changes in climate teleconnections and GRACE TWS variability, we applied the one-dimensional CSEOF (CSEOF-1D; SI, section 2.2) [42, 43] to the time series of the climate indices and detrended GRACE TWS variability (i.e. subtracted linear trend) at a nested 12 month period (tables S23, S24). CSEOF provides independent interpretable modes with the percentage of explained variance. We selected Principal Component Timeseries (PCT) from the reconstructed variable modes that explain 97% of the total variance of the original time series. These PCTs include the modulated annual cycle and interannual to decadal variations. Cross-correlations between bivariate PCTs were evaluated with a lag of ≤ 36 months (table S25).

2.3. Land cover and vegetation index

Impacts of irrigation on water use in northern Africa were evaluated using land cover dynamics (table S26). The proportion of arable land under irrigation in SSA is less than 5% [44]. Because irrigation is the primary driver of GW pumpage in many regions, with limited irrigation we would not expect intensive GW pumpage throughout much of the African continent outside of north Africa. Vegetation indices are also a very powerful indicator of climate extremes. We evaluated time series of NDVI (table S22, SI, sections 1.3 and 2.3) [45].

2.4. Groundwater storage variability

Although this study focuses primarily on GRACE TWS variability, we calculated GWS variability from TWS variability by subtracting modeled soil moisture storage (SMS from CLSM-F2.5, NOAA-4.6, and VIC 4.0.3 models) in the major aquifers (table S16) [46]. GRACE TWS anomalies include water storage in shallow and deep aquifers; however, separating these two systems is extremely complicated and would require extensive *in-situ* monitoring data, which are difficult to obtain in Africa. We evaluated Surface Water Storage Anomalies (SWSAs) computed as the accumulated runoff in GLDAS models (table S29); however, these values were very low, and we did not consider them in the final analysis.

3. Results and discussion

3.1. Long-term variability in GRACE total water storage

GRACE recorded declining apparent TWS trends in northern Africa and low trends or rising trends in the remaining aquifers throughout the continent (figure 2, S1 (available online at stacks.iop.org/ERL/17/014046/mmedia)). One of the main questions is

whether these apparent trends reflect natural climate variability or longer-term secular trends, suggesting persistence and predictive skill. Declining linear trends in the northern African aquifers (Nubian Aquifer System [NAS], NW Sahara: trends: -60 to -73 km³ over the 18 yr GRACE/FO record) could persist with linear trends dominating TWS variance (68%–81%, figure S2), good fits for linear trends with high R² values (0.77–0.88), and trend magnitudes greatly exceeding the SD of interannual variability (TIVR: -10 to -84) (figure S3, table 1). The declining linear trend in the NAS extended from 2002 to 2013 and TWSAs stabilized after 2013.

TWS linear trends were close to 0 in some aquifers (Taoudeni, Umm Rawaba, L Kalahari, and Karoo) (figure 2, S1, table 1). In contrast, apparent TWS trends were rising in many other African aquifers (Senegal, Iullemeden, Lake Chad, Ogaden-Juba, Congo, and Upper Kalahari: 23–131 km³ over 18 yr). The highest apparent TWS trend was found in the U Kalahari. The linear trends in some western African aquifers (Senegal and Iullemeden) are likely to persist, based on high R² (0.79–0.87) and high positive TIVRs (6–10), indicating that the trends greatly exceed interannual variability (figure S3, table 1).

Apparent TWS trends outside of northern and western African aquifers reflect predominantly interannual climate variability based on TWS linear trends accounting for low to moderate percentages of TWS variance (0.0%–22%), poor fits of linear trends (mostly low R² values: 0.01–0.38), and linear trends mostly within ± 2 SDs of interannual variability (TIVR: -0.8 to 2.3) (table 1, S1(a, b), figure S3). Therefore, the apparent trends, even though large in magnitude in some aquifers (e.g. Congo and U Kalahari) have little predictive skill. Interannual variability is low in aquifers in northern and western Africa (SD: 5–9 mm) and is generally much higher in aquifers throughout the rest of Africa (SD: 12–88 mm), highest in the Upper Kalahari aquifer (table 1). Interannual variance in TWS as a percentage of the total variance is highest in southern Africa (Karoo and Lower Kalahari aquifers, 56%–80% of total TWS variance) and in eastern Africa (Ogaden Juba aquifer: 47% of variance). Interannual and annual variances in TWS are almost equally important in the Upper Kalahari, whereas annual variance dominates in aquifers close to the Equator (Congo, Lake Chad, and Umm Ruwaba, 49%–79% of TWS variance) (figure S2).

3.2. Comparison of total water storage and groundwater storage

Although this study emphasizes TWS variability, we also compared GWS to TWS variability because of the high contribution of GWS to TWS trends [41, 47] and many studies focus on GWS variability [10, 12]. Time series of TWS and GWS are highly correlated in

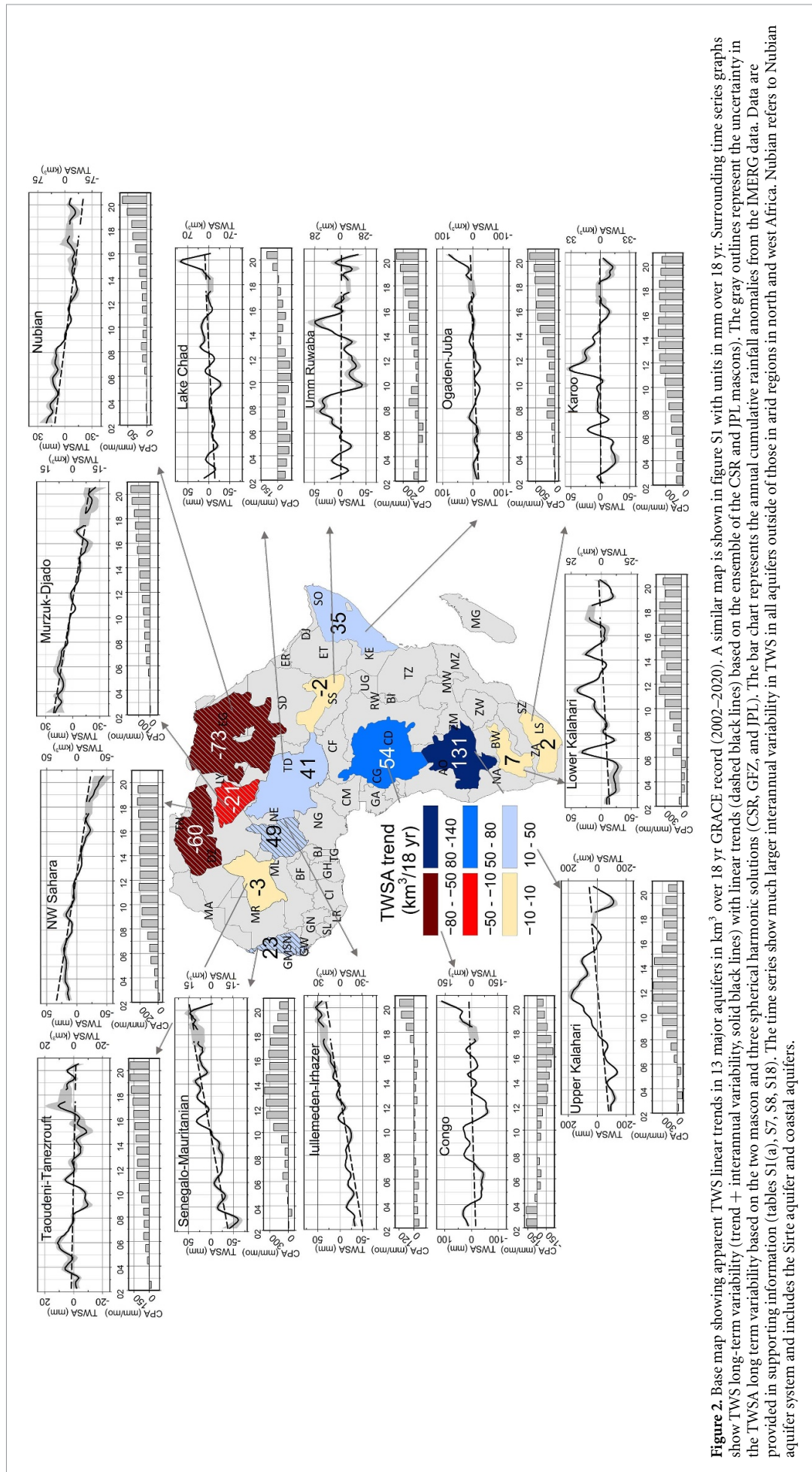


Figure 2. Base map showing apparent TWS linear trends in 13 major aquifers in km³ over 18 yr GRACE record (2002–2020). A similar map is shown in figure S1 with units in mm over 18 yr. Surrounding time series graphs show TWS long-term variability (trend + interannual variability, solid black lines) with linear trends (dashed black lines) based on the ensemble of the CSR and JPL mascons). The gray outlines represent the uncertainty in the TWSA long term variability based on the two mascon and three spherical harmonic solutions (CSR, GFZ, and JPL). The bar chart represents the annual cumulative rainfall anomalies from the IMERG data. Data are provided in supporting information (tables S1(a), S7, S8, S18). The time series show much larger interannual variability in TWS in all aquifers outside of those in arid regions in north and west Africa. Nubian refers to Nubian aquifer system and includes the Sirte aquifer and coastal aquifers.

most aquifers ($R = \sim 0.70\text{--}1.0$), with the exception of the Lower Kalahari ($R = 0.56$) and Karoo ($R = 0.58$) (table 1). Relationships between TWS and GWS variability depend mostly on simulated SMS. Aquifers where TWS and GWS variability do not align well show large differences in simulated SMS between the two LSMs used in this analysis (CLSM and NOAH). For example, simulated SMS in CLSM is much less variable than that from NOAH with standard deviations in CLSM SMS ranging from $\sim 15\%$ to $\sim 30\%$ of those from NOAH in the aquifers where TWS and GWS variabilities do not align (table S1(g)). Therefore, differences between TWS and GWS variability may reflect uncertainties in simulated SMS.

3.3. Causes of total water storage variability

3.3.1. Human intervention

TWS variability in northern African aquifers is linked to natural long-term decline from previous pluvial periods and human intervention [18]. The Nubian Aquifer is a fossil aquifer that was recharged during past glacial periods more than 5000–10 000 yr ago with storage declining naturally with climate change from the Pleistocene to the Holocene period [48]. Human intervention is the dominant factor driving declining TWS trends in these aquifers; however, available data on water use are limited. Simulated net GW abstraction using WGHM is lower than declines estimated by GRACE: NAS: WGHM, $-2.7 \text{ km}^3 \text{ yr}^{-1}$ vs. GRACE: $\sim -4.0 \text{ km}^3 \text{ yr}^{-1}$; NW Sahara aquifer: WGHM, $-1.7 \text{ km}^3 \text{ yr}^{-1}$ vs. GRACE: $\sim -3.3 \text{ km}^3 \text{ yr}^{-1}$ (table 1). The NAS includes Lake Nasser with water storage anomalies mainly controlled by interannual variations in the Nile flow and could contribute to the TWS trend during dry/wet cycles. Lake Nasser storage declined by $\sim 30 \text{ km}^3$ (altimetry, 2002–2013; table S12). Applying this depletion to the entire NAS suggests that Lake Nasser would contribute $\sim 36\%$ to the TWS trend in the NAS. A recent study assessing Lake Nasser impacts on NAS using forward modeling [49] indicates that Lake Nasser would contribute $\sim 16\%$ – 17% of TWS depletion in the NAS (table S12).

Regional modeling of the NAS indicates that pumpage totaled $\sim 2.3 \text{ km}^3$ in 1998, also less than the GRACE data, and mostly from Egypt (45%) and Libya (37%) [48]. Libya constructed the Great Man-made River (GMR) project, designed to transfer $\leq 2.2 \text{ km}^3 \text{ yr}^{-1}$ from the NAS to the north for irrigation ($\sim 80\%$) and to coastal cities (e.g. Benghazi, Tripoli, etc) but GMR has not been operating at capacity since the 2011 war [50]. Recent recharge estimates suggest low rates in the NAS that would represent $\sim 5\%$ of the TWS depletion [17]. Although irrigated areas in northern African aquifers represent only $\sim 0.2\%$ – 2% of the total land area, vegetated areas delineated by satellite data have increased by 17% – $\sim 90\%$ from 2001 to 2019 (table S26),

suggesting increased irrigation and related water abstraction (table S1(h)). GW discharge may be even greater if we consider natural discharge from oases (e.g. El Kharga, EL Baheriya, Siwa, El—Dakhla).

TWS trends in some west African aquifers (e.g. Iullemeden) may also be related to human intervention. Previous studies indicate that land use change from deep rooted shrubland to shallow rooted cropland resulted in rising GW recharge, increasing TWS [14]. This is supported by rising GW levels (figure S4) and by a previous GRACE study [10, 15].

3.3.2. Climate and climate teleconnections

TWS variability (detrended) is moderately to highly correlated with monthly precipitation anomalies (IMERG) in most aquifers ($R = 0.56\text{--}0.87$) with lags of 1–3 months that may reflect the time for water storage to accumulate (tables 1, S1(c)). Exceptions include aquifers in northern Africa ($R = 0.15\text{--}0.33$, lags 3–14 mos), Taoudeni in central Africa ($R = 0.24$), and Karoo in southern Africa ($R = 0.28$). Focusing on interannual TWS variability alone relative to cumulative monthly precipitation anomalies results in low correlations in most aquifers, except for the Kalahari and Karoo aquifers ($R = 0.48\text{--}0.82$; table 1), indicating longer term precipitation memory in these aquifers, also noted in previous studies [10, 51].

Assessing linkages between TWS variability and NDVI provides a further test of the relationship between climate and TWS variability as precipitation and NDVI are highly correlated in many regions. Maximum cross correlations between TWS variability (detrended) and NDVI (without climatology), considering lag effects, are low in aquifers in northern Africa ($R = 0.00\text{--}0.36$), consistent with poor relationships between TWS variability and climate forcing in these aquifers (table 1, figure S5). Most of the remaining aquifers have moderate to high cross correlations between variability in TWS and NDVI ($R: 0.45\text{--}0.70$), further emphasizing the importance of climate as a driver of TWS variability in these aquifers.

Discussion of climate teleconnections and TWS variability focuses on eastern and southern Africa only (figures 3–6) because TWS variability in northern and western African aquifers is dominated by long-term trends. Variances in interannual and annual TWS only account for 2%–16% of total variance in TWS in these northern and western aquifers (table S1(a)). However, cross-correlations between climate teleconnections and TWS variability are provided for all aquifers based on CSEOF analysis (figure S8).

Some of the most important teleconnections in Africa include ENSO and IOD. ENSO exhibits a strong dipole between eastern Africa and southern Africa [33, 52]. El Nino is linked to mostly wet conditions in eastern Africa and dry conditions in

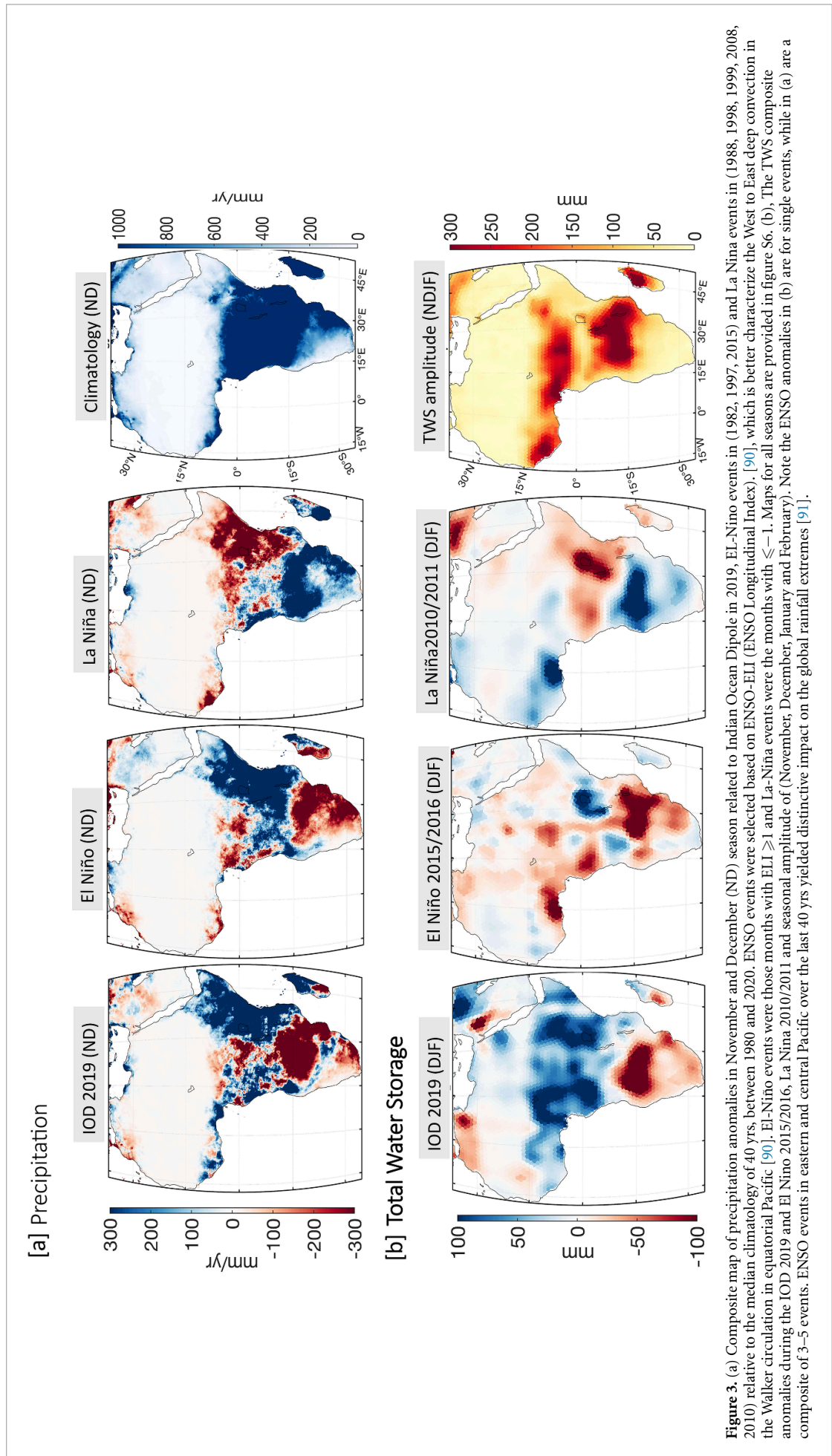
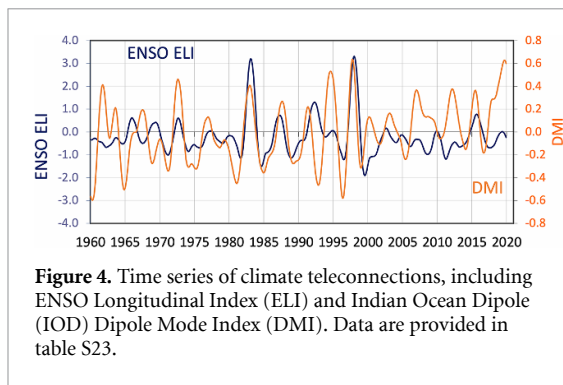


Figure 3. (a) Composite map of precipitation anomalies in November and December (ND) season related to Indian Ocean Dipole in (1982, 1997, 2015) and La Niña events in (1988, 1998, 1999, 2008, 2010) relative to the median climatology of 40 yrs, between 1980 and 2020. ENSO events were selected based on ENSO-ELI (ENSO Longitudinal Index). [90], which is better characterize the West to East deep convection in the Walker circulation in equatorial Pacific [90]. El-Niño events were those months with $ELI \geq 1$ and La-Niña events were the months with $ELI \leq -1$. Maps for all seasons are provided in figure S6. (b). The TWS composite anomalies during the IOD 2019 and El Niño 2015/2016, La Niña 2010/2011 and seasonal amplitude of (November, December, January and February). Note the ENSO anomalies in (b) are for single events, while in (a) are a composite of 3–5 events. ENSO events in eastern and central Pacific over the last 40 yrs yielded distinctive impact on the global rainfall extremes [91].



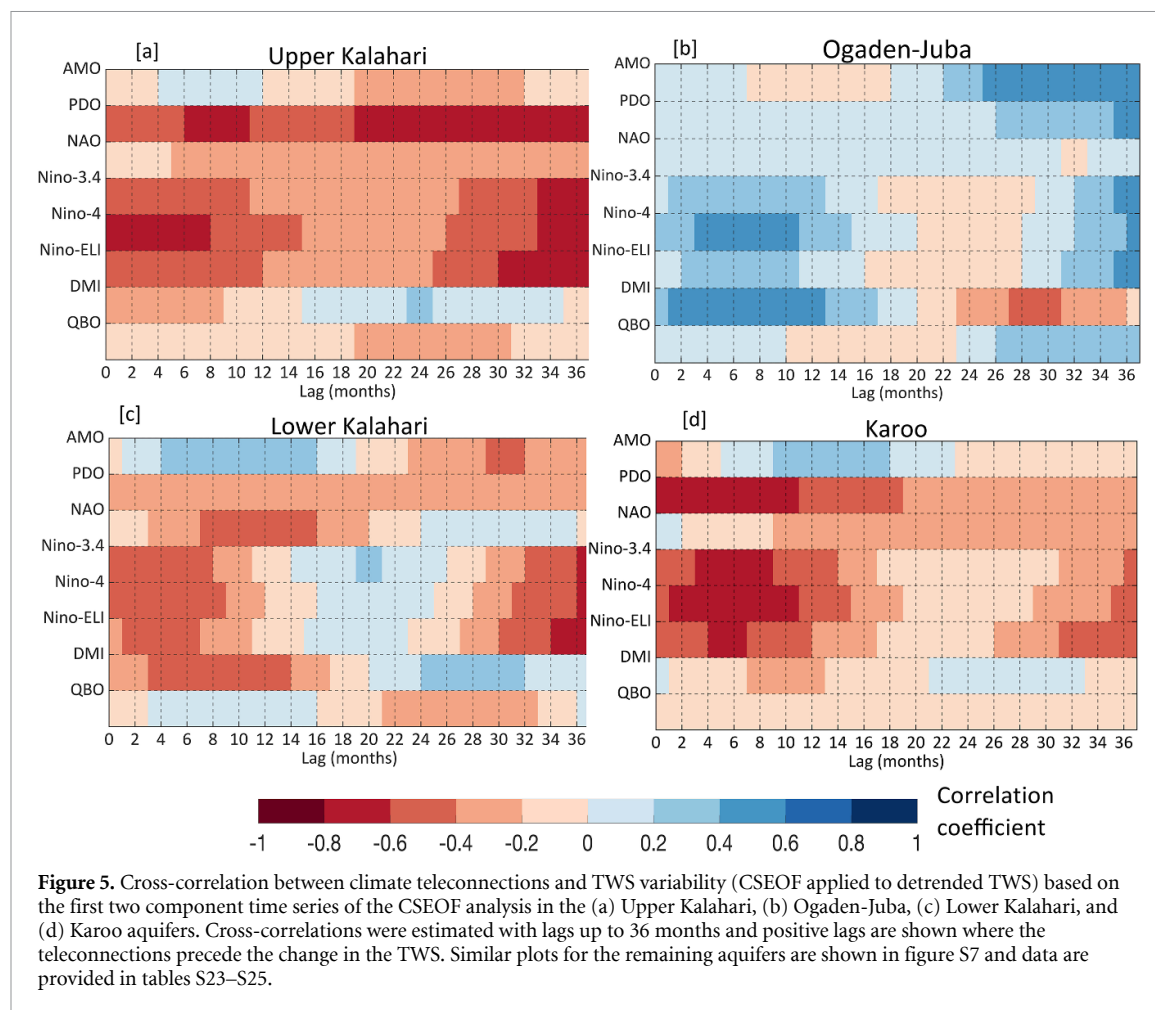
southern Africa, with the opposite relationship during La Nina, as shown by seasonal rainfall in Nov–Dec (figure 3) [24, 25]. These variations in rainfall are related to corresponding variations in GRACE-derived TWS anomalies. During the 2015–2016 El Nino; however, central and northern Ethiopia (latitudes 7° – 14°) witnessed one of the worst droughts in 50 years during the JJAS dry season, and extended to wet season in DJF [53, 54]. The DJF season in southern Africa during this ENSO event was also extremely dry [22] (figure 3). The IOD is also important with impacts on rainfall and TWS similar to those of ENSO in eastern Africa extending to western Africa. Conditions in the Indian and Pacific oceans were synchronized during some periods (e.g. 1982–1983; 1997–1998) (figure 5). The recent 2019 IOD resulted in extreme rainfall over eastern and central Africa and led to increases in TWS during November–December (ND) 2019—January/February (JF) 2020 (figure 3).

Eastern Africa, including the Horn of Africa, is repeatedly subjected to floods and droughts. Inter-annual variability in TWS in the Ogaden Juba aquifer is positively correlated with El Nino (Nino-4) ($R = 0.42$ – 0.47 ; minimum lag \sim three months) (figure 5(b)). Although the 2015–2016 strong El Nino was projected to cause intense precipitation, precipitation data show moderate impacts [55] (figure 3) and are consistent with limited variability in the TWS time series in the Ogaden Juba aquifer (figure 2). SPEI data also reveal short mild to moderate wet conditions during 2015–2016 El Nino in the Ogaden Juba aquifer (figure 6(b)). In this aquifer, drought conditions occurred in the following La Nina in 2017, which extended throughout the Horn of Africa, resulting in widespread food insecurity. This drought was followed by flooding in 2018 (MAM rainy season), as seen in the Shebelle and Juba rivers (figure S10) and in much of Kenya [56] and the Horn of Africa [57]. Drought occurred in this region in early 2019 (figure 6(b)) and was followed by intense rainfall in October to December (2019) due to the warm conditions in the Indian Ocean (IOD) (figure 3). The strong positive IOD increased TWS by $\sim 20 \text{ km}^3$ in the Ogaden-Juba aquifer and resulted in intensive flooding over eastern Africa and the Horn of Africa,

adversely impacting 2.8 million people [58, 59]. Lake Victoria levels increased markedly in response to IOD (figure S11). In general, TWS variability in the Ogaden Juba aquifer was more highly impacted by IOD than ENSO based on the cross correlation between TWS variability and the IOD Dipole Mode Index (DMI: $R = 0.50$ – 0.56) with a lag of ~ 3 mos (figure 5(b)). However, outside of the Ogaden Juba aquifer, particularly in Ethiopia, there were strong drought responses to the 2015–2016 El Nino [22, 60]. Climate-driven reconstructed TWS variability in the Ogaden Juba aquifer shows a large increase ($\sim 50 \text{ km}^3$) related to the 1997/1998 El Nino (figure S12(a)), the strongest in the last century followed by a rapid decline in TWS in response to the following La Nina in 1998–2000. Reservoir storage provides additional information showing a large increase in Lake Victoria in 1997/1998 (figure S11).

In southern Africa, TWS variability in the Karoo aquifer is negatively correlated with ENSO (ENSO 3.4, 4.0, and ELI; $R = -0.71$ to -0.54 : short lag) (figure 5(d)) as expected based on linkages between ENSO and precipitation [22]. SPEI data reveal drought conditions during El Nino (2015–2016) followed by slightly wetter conditions in 2016 (figure 6(d)). Declining TWS in the Karoo aquifer in 1997/1998 is consistent with a negative correlation between ENSO and TWS (figure S12(b)). TWS variability in the Kalahari (L and U) aquifers is also negatively correlated with ENSO (3.4 and 4.0) ($R = \sim -0.5$ to ~ -0.60) with short lags (figures 6(a) and (c)). TWS in the Karoo and Kalahari aquifers peaked in 2011, corresponding to La Nina; however, TWS was building up over the long term prior to 2011 (figure 2). Wet conditions during the 2011 La Nina are also evident in the SPEI and NDVI data for the Karoo and Kalahari aquifers (figures 3 and 6). These aquifers display longer term trends in reconstructed TWS variability, peaking in the mid-1970s followed by a decline in TWS (figure S12(b)). The mid-1970s TWS change corresponds to a climate regime shift that has been linked to Interdecadal Pacific Oscillation (IPO) in previous studies [61, 62]. Although the Cape Town region in the southwest portion of South Africa also experienced severe drought in 2015/2017, the drivers were different in this region [63]. Low-frequency teleconnections (e.g. PDO, AMO) impact TWS variability in this region of South Africa. TWS variability in both U Kalahari and Karoo is negatively correlated with PDO ($R = -0.65$ – 0.68 , lags 5–28 months) (figure 5).

Additional hydrologic data at local and regional scales would help fine-tune future estimates of GWS, trends, and potential in Africa and for comparison with GRACE data. Expansion of the limited GW level monitoring data that are reported by the International Groundwater Resources Assessment Centre (IGRAC) would help with understanding the dynamics of GW storage in Africa (figure S16).



Groundwater level monitoring is clustered in certain countries, such as South Africa [64], Burkina Faso [65], and Uganda [66]. Previous regional-scale studies have evaluated representative long-term GW level hydrographs [67]. Pumping-test data would also be helpful for quantifying storage coefficients of different aquifers but the quality, quantity, and duration of these tests, commonly conducted at the commissioning of boreholes, rather than careful experiments are limited [68].

3.4. Implications for water resources management

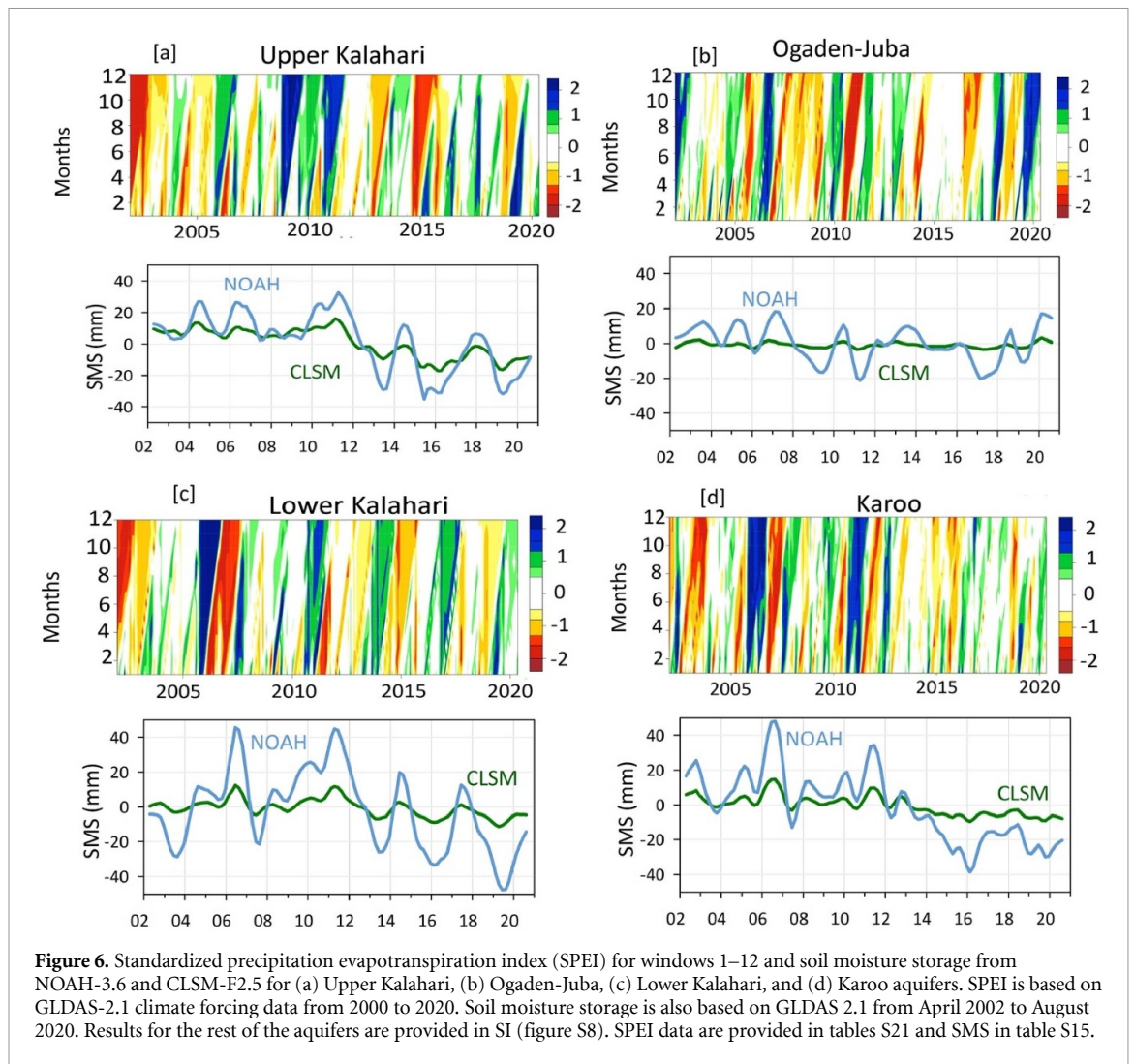
The results of this study have implications for how water is managed, considering the measurable impact on water storage of human intervention through GW abstraction in northern Africa, land use change in western Africa, and climate variability and teleconnections, particularly in eastern and southern Africa. Differences in drivers of water storage variability underscore the need to develop different water management strategies in various regions.

One of the primary issues for water managers is the repeated wet and dry climate cycles that impact water resources in the form of extreme droughts and floods. However, water storage variability is often not considered in planning analyses, which generally rely on long-term water balance. This study highlights the

importance of considering climate/hydrological variability in planning for future water investments. A variety of approaches can be used to adapt to these extremes, with access to increased water storage seen as one of the ways that physical water security can be improved [69] amongst a much more complex web of physical and social processes [70]. Water storage changes reflect the balance between inputs and outputs, or replenishment relative to demands:

$$\begin{aligned} &\text{Input(replenishment)} - \text{Output(demands)} \\ &= \text{Change in water storage.} \end{aligned}$$

More climate resilient water management can be accomplished by storing water from wet to dry climate cycles, transporting water from wet to dry regions, adopting different technologies for water supplies and/or reducing water demands [71]. For many, water storage is synonymous with lakes or reservoirs, such as the Great African Lakes, Lake Nasser and the Grand Ethiopian Renaissance Dam (figure S11) and water transfer with large rivers, such as the Nile, Niger or Zambezi, or interbasin transfer schemes in southern Africa. However, GWS in the continent (~ 0.66 million km^3) exceeds SW storage estimates by ~ 20 times², and annual GW recharge (1500 km^3) is equivalent to the combined annual



flow in the Congo, Nile, Niger, and Zambezi rivers [17]. Therefore, accessing the natural water storage provided by aquifers in Africa is the obvious way to manage the variability between droughts and floods.

Recharge rates are generally inversely related to aquifer storage in Africa, with low recharge rates (mostly prior to 5000 yr ago) in aquifers with large storage in northern Africa relative to higher recharge rates in low storage aquifers throughout much of the rest of Africa (figure 7) [17]. The small negative storage trends in the northern African aquifers are insignificant compared to the overall storage within these aquifers and there is little chance that current abstraction will lead to significant regional depletion, as shown by previous regional modeling [48]. However, this does not mean that depletion does not have an impact locally. Continued depletion leads to falling GW levels, locally reducing discharge to oases, causing failure of some shallow wells, and increasing pumping costs [48].

In western African aquifers, where GW levels have been rising due to land use change, GW may need to be managed to reduce GW flooding or waterlogging and subsequent salinization. This has also occurred in

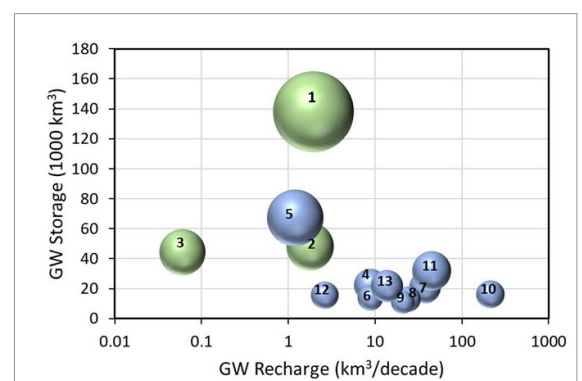


Figure 7. Relationship between mean absolute GW storage and decadal GW recharge in major Africa aquifers (table S1(e)). Aquifers colored green are in northern Africa (1. Nubian Aquifer System; 2. NW Sahara; 3. Murzuk-Djado) and rest of Africa (4. Senegalo; 5. Taoudeni; 6. Iullemeden; 7. Lake Chad; 8. Umm Ruwaba; 9. Ogaden-Juba; 10. Congo; 11. U Kalahari; 12. L Kalahari; and 14. Karoo [17]). Aquifers with large storage generally have low recharge rates.

parts of the Indo-Gangetic basin with increased GW recharge due to SW irrigation having to be carefully managed through dedicated long-term drilling and drainage programs.

Eastern and southern African aquifers have both significant GWS and evidence of long-term GW recharge. The periodic nature of TWS variations, as evidenced from GRACE, highlights the feasibility of conjunctive use of SW and GW. The large GWS volumes can be used in dry cycles with the knowledge that significant rainfall is likely to occur in the coming decades linked to global climate teleconnections which will both recharge the GW systems and enable SW to be used for irrigation and water supply.

Although irrigation in Africa relies primarily on SW [72]; conjunctive use of SW and GW has been increasing in the Nile Valley (Sudan/Egypt) [73, 74], Ethiopia (Lake Tana Basin) [75], and the Orange River in South Africa (figure S14). Groundwater is often used conjunctively with SW in urban water supply, both through municipal supply (e.g. Nairobi, Addis Ababa) [76, 77] and more commonly as informal private supply to supplement unreliable piped schemes [76, 78]. People have developed techniques for increasing small scale water storage in Africa for millennia. Haffirs are used in Ethiopia for rainwater harvesting and are surrounded by bunds to store excess rainwater for later use during droughts. These systems can range in size, storing from 30 000 to 100 000 m³. Stone terracing and soil bunds are well-known approaches to reduce soil erosion during flooding but have the added benefit of enhancing GW recharge, as shown by watersheds in Ethiopia [79]. Development of Managed Aquifer Recharge (MAR) projects is still very limited in Africa with a recent review reporting a total of 52 systems, with most in South Africa (17 systems), Tunisia (11) and Kenya (8) [80]. Water for MAR is sourced primarily from SW and infiltration is done using spreading basins, in channel sand dams in Kenya, and shafts and boreholes in South Africa. Spate irrigation has also been shown to enhance GW sustainability by spreading out flood waters onto adjacent riverbanks to improve water storage and irrigated agriculture, as discussed for Ethiopia [81]. Drilling wells in ephemeral channels would also take advantage of recharge during flooding periods, as shown by examples in Kenya [82]. Extracting GW near SW bodies may essentially be capturing SW and should help with conjunctive use as long as SW is not adversely impacted, such as intensive irrigation along sections of the Orange River (figure S14). Additional examples include the Rift Valley (Lake Naivasha, Kenya [83], and Lake Ziway, Ethiopia [84]), and the Nile Delta [85].

Drought resiliency can be enhanced by diversifying and increasing access to water supplies. For example, the city of Cape Town (population ~4 million) relied almost entirely on SW prior to the 2015–2017 drought, based on six reservoirs (figure S15). As drought intensified, emergency measures to reduce demand had to be introduced, alongside drilling of emergency boreholes and installation of temporary desalination plants to increase supplies.

Further research shows that GW can provide a long-term solution to increasing drought resilience for Cape Town, including Table Mountain, Atlantis, and Malmesbury aquifers [86, 87]. Recent research of the 2015–2016 drought in Ethiopia demonstrated that having access to GW dramatically increased water security for rural villages, as measured by time taken to collect water, water use, conflict, and school attendance [88]. A national survey of water supply performance in Ethiopia demonstrated that in priority districts, GW supplies outperformed other water supply options during drought [89]. Therefore, most initiatives to increase the resilience of community water supplies to drought rely on increasing access to GW.

4. Conclusions

- (a) GRACE TWS variability from 2002 to 2020 was dominated by long-term trends in northern and western Africa and by interannual variability outside of these regions, with highest interannual variability in the Upper Kalahari aquifer.
- (b) Variations in TWS were controlled by human intervention in northern Africa (mostly groundwater abstraction for irrigation in Nubian and NW Sahara aquifers) and in western Africa, with increased storage related to recharge from land use change (particularly in the Iullemeden aquifer).
- (c) Climate extremes and teleconnections control interannual variability in TWS in eastern and southern Africa. ENSO is generally linked to wet conditions in the Ogaden Juba aquifer in eastern Africa and dry conditions in the Karoo aquifer in southern Africa. The 2015/2016 El Nino did not have a large impact in the Ogaden Juba aquifer in eastern Africa but resulted in extensive drought in other parts of eastern Africa and in southern Africa. The IOD resulted in extensive flooding in eastern Africa in 2019–2020. Reconstructed TWS variability shows strong impacts of 1997–1998 El Nino with dipole effects in eastern and southern Africa. These climate cycles result in repeated droughts and floods in these regions.
- (d) Managing these climate extremes can be accomplished by making better use of GWS, conjunctively managing SW (mostly during wet cycles) and GW (primarily during droughts), increasing access to boreholes, and promoting other technologies where appropriate (e.g. managed aquifer recharge, desalination).

Data availability statement

The data that support the findings of this study are openly available at the following URL/DOI: <https://dataverse.tdl.org/dataset.xhtml?persistentId=doi:10.18738/T8/HLXCMY>

All data that support the findings of this study are included within the article (and any supplementary files).

Acknowledgments


We would like to acknowledge support from the Jackson Endowment at the University of Texas at Austin to conduct this study.

ORCID iDs

Bridget R Scanlon  <https://orcid.org/0000-0002-1234-4199>

Ashraf Rateb  <https://orcid.org/0000-0002-8875-1508>

Alan M MacDonald  <https://orcid.org/0000-0001-6636-1499>

Mohammad Shamsudduha  <https://orcid.org/0000-0002-9708-7223>

Alexander Sun  <https://orcid.org/0000-0002-6365-8526>

Richard G Taylor  <https://orcid.org/0000-0002-9867-8033>

References

- [1] UNICEF/ WHO 2019 *Progress on household drinking water, sanitation and hygiene I 2000-2017* (New York: United Nations Children's Fund (UNICEF) and World Health Organization) p 140
- [2] MacDonald A M, Bonsor H C, Dochartaigh B E O and Taylor R G 2012 Quantitative maps of groundwater resources in Africa *Environ. Res. Lett.* **7** 024009
- [3] Kundzewicz Z W and Döll P 2009 Will groundwater ease freshwater stress under climate change? *Hydrol. Sci. J.* **54** 665–75
- [4] Cobbing J 2020 Groundwater and the discourse of shortage in sub-Saharan Africa *Hydrogeol. J.* **28** 1143–54
- [5] Wu G C *et al* 2017 Strategic siting and regional grid interconnections key to low-carbon futures in African countries *Proc. Natl Acad. Sci.* **114** E3004–12
- [6] Hartung H and Pluschke L 2018 *Food and Agricultural Organization* 978-92-5-130479-2 FAO p
- [7] Ahmed M, Sultan M, Wahr J and Yan E 2014 The use of GRACE data to monitor natural and anthropogenic induced variations in water availability across Africa *Earth Sci. Rev.* **136** 289–300
- [8] Grippa M *et al* 2011 Land water storage variability over West Africa estimated by Gravity Recovery and Climate Experiment (GRACE) and land surface models *Water Resour. Res.* **47** W05549
- [9] Rodell M *et al* 2018 Emerging trends in global freshwater availability *Nature* **557** 651–9
- [10] Bonsor H C, Shamsudduha M, Marchant B P, MacDonald A M and Taylor R G 2018 Seasonal and decadal groundwater changes in African sedimentary aquifers estimated using GRACE products and LSMs *Remote Sens.* **10** 904
- [11] Frappart F 2020 Groundwater storage changes in the major North African transboundary aquifer systems during the GRACE era (2003–2016) *Water* **12** 2669
- [12] Shamsudduha M and Taylor R G 2020 Groundwater storage dynamics in the world's large aquifer systems from GRACE: uncertainty and role of extreme precipitation *Earth Syst. Dyn.* **11** 755–74
- [13] Vishwakarma B D, Bates P, Sneeuw N, Westaway R M and Bamber J L 2020 Re-assessing global water storage trends from GRACE time series *Environ. Res. Lett.* **16** 034005
- [14] Favreau G *et al* 2009 Land clearing, climate variability, and water resources increase in semiarid southwest Niger: a review *Water Resour. Res.* **45** W00A16
- [15] Cuthbert M O *et al* 2019 Observed controls on resilience of groundwater to climate variability in sub-Saharan Africa *Nature* **572** 230
- [16] Jasechko S and Taylor R G 2015 Intensive rainfall recharges tropical groundwaters *Environ. Res. Lett.* **10** 124015
- [17] MacDonald A M *et al* 2021 Mapping groundwater recharge in Africa from ground observations and implications for water security *Environ. Res. Lett.* **16** 034012
- [18] Gossel W, Ebraheem A M and Wycisk P 2004 A very large scale GIS-based groundwater flow model for the Nubian sandstone aquifer in eastern Sahara (Egypt, northern Sudan and eastern Libya) *Hydrogeol. J.* **12** 698–713
- [19] Werth S, White D and Bliss D W 2017 GRACE detected rise of groundwater in the Sahelian Niger River Basin *J. Geophys. Res.: Solid Earth* **122** 10459–77
- [20] Awange J L *et al* 2008 The falling Lake Victoria water level: GRACE, TRIMM and CHAMP satellite analysis of the lake basin *Water Resour. Manage.* **22** 775–96
- [21] Shamsudduha M *et al* 2017 Recent changes in terrestrial water storage in the Upper Nile Basin: an evaluation of commonly used gridded GRACE products *Hydrol. Earth Syst. Sci.* **21** 4533–49
- [22] Kolusu S R *et al* 2019 The El Nino event of 2015–2016: climate anomalies and their impact on groundwater resources in East and southern Africa *Hydrol. Earth Syst. Sci.* **23** 1751–62
- [23] Nicholson S E 2014 Spatial teleconnections in African rainfall: a comparison of 19th and 20th century patterns *Holocene* **24** 1840–8
- [24] Funk C *et al* 2019 Recognizing the famine early warning systems network: over 30 years of drought early warning science advances and partnerships promoting global food security *Bull. Am. Meteorol. Soc.* **100** 1011–27
- [25] Nicholson S E, Funk C and Fink A H 2018 Rainfall over the African continent from the 19th through the 21st century *Glob. Planet Change* **165** 114–27
- [26] Anyah R O, Forootan E, Awange J L and Khaki M 2018 Understanding linkages between global climate indices and terrestrial water storage changes over Africa using GRACE products *Sci. Total Environ.* **635** 1405–16
- [27] Awange J L, Forootan E, Kuhn M, Kusche J and Heck B 2014 Water storage changes and climate variability within the Nile Basin between 2002 and 2011 *Adv. Water Resour.* **73** 1–15
- [28] Awange J L, Schumacher K M, Forootan E and Heck B 2016 Exploring hydro-meteorological drought patterns over the Greater Horn of Africa (1979–2014) using remote sensing and reanalysis products *Adv. Water Resour.* **94** 45–59
- [29] Khaki M, Awange J, Forootan E and Kuhn M 2018 Understanding the association between climate variability and the Nile's water level fluctuations and water storage changes during 1992–2016 *Sci. Total Environ.* **645** 1509–21
- [30] Ndehedehe C E, Awange J L, Corner R J, Kuhn M and Okwuashi O 2016 On the potentials of multiple climate variables in assessing the spatio-temporal characteristics of hydrological droughts over the Volta Basin *Sci. Total Environ.* **557** 819–37
- [31] Ndehedehe C E, Awange J L, Kuhn M, Agutu N O and Fukuda Y 2017 Analysis of hydrological variability over the Volta river basin using *in-situ* data and satellite observations *J. Hydrol.: Reg. Stud.* **12** 88–110
- [32] Anyamba A, Tucker C J and Eastman J 2001 NDVI anomaly patterns over Africa during the 1997/98 ENSO warm event *Int. J. Remote Sens.* **22** 1847–59
- [33] Anyamba A, Glennie E and Small J 2018 Teleconnections and interannual transitions as observed in African vegetation: 2015–2017 *Remote Sens.* **10** 1038

- [34] Ramillien G, Frappart F and Seoane L 2014 Application of the regional water mass variations from GRACE satellite gravimetry to large-scale water management in Africa *Remote Sens.* **6** 7379–405
- [35] Swenson S and Wahr J 2009 Monitoring the water balance of Lake Victoria, East Africa, from space *J. Hydrol.* **370** 163–76
- [36] Resende T C *et al* 2019 Assessment of the impacts of climate variability on total water storage across Africa: implications for groundwater resources management *Hydrogeol. J.* **27** 493–512
- [37] Humphrey V, Gudmundsson L and Seneviratne S I 2017 A global reconstruction of climate-driven subdecadal water storage variability *Geophys. Res. Lett.* **44** 2300–9
- [38] Wiese D N, Landerer F W and Watkins M M 2016 Quantifying and reducing leakage errors in the JPL RL05M GRACE mascon solution *Water Resour. Res.* **52** 7490–502
- [39] Save H, Bettadpur S and Tapley B D 2016 High-resolution CSR GRACE RL05 mascons *J. Geophys. Res. Solid Earth* **121** 7547–69
- [40] Cleveland R B, Cleveland W S and Terpenning I 1990 STL: a seasonal-trend decomposition procedure based on loess *J. Off. Stat.* **6** 3
- [41] Scanlon B R, Rateb A, Pool D, Stanfrod W, Save H, Sun A, Long D and Fuchs B 2021 Effects of climate and irrigation on GRACE-based estimates of water storage changes in major US aquifers *Environ. Res. Lett.* **16** 094009
- [42] Kim K-Y and North G R 1997 EOFs of harmonizable cyclostationary processes *J. Atmos. Sci.* **54** 2416–27
- [43] Kim K-Y and Wu Q 1999 A comparison study of EOF techniques: analysis of nonstationary data with periodic statistics *J. Clim.* **12** 185–99
- [44] Villholth K G 2013 Groundwater irrigation for smallholders in sub-Saharan Africa—a synthesis of current knowledge to guide sustainable outcomes *Water Int.* **38** 369–91
- [45] Didan K 2021 MOD13Q1 MODIS/Terra Vegetation Indices 16-Day L3 Global 250m SIN Grid V006 [Data Set] NASA EOSDIS Land Processes DAAC. 2015 2021-05-30
- [46] Koster R D, Suarez M J and Heiser M 2000 Variance and predictability of precipitation at seasonal-to-interannual timescales *J. Hydrometeorol.* **1** 26–46
- [47] Rateb A *et al* 2020 Comparison of groundwater storage changes from GRACE satellites with monitoring and modeling of major U.S. aquifers *Water Resour. Res.* **56** e2020WR027556
- [48] Voss C I and Soliman S M 2014 The transboundary non-renewable Nubian Aquifer System of Chad, Egypt, Libya and Sudan: classical groundwater questions and parsimonious hydrogeologic analysis and modeling *Hydrogeol. J.* **22** 441–68
- [49] Deggim S *et al* 2021 RECOG RL01: correcting GRACE total water storage estimates for global lakes/reservoirs and earthquakes *Earth Syst. Sci. Data* **13** 2227–44
- [50] Brika B 2018 Water resources and desalination in Libya: a review *Proceedings* **2** 586
- [51] Opie S, Taylor R G, Brierley C M, Shamsudduha M and Cuthbert M O 2020 Climate-groundwater dynamics inferred from GRACE and the role of hydraulic memory *Earth Syst. Dyn.* **11** 775–91
- [52] Funk C *et al* 2018 Examining the role of unusually warm Indo-Pacific sea-surface temperatures in recent African droughts *Q. J. R. Meteorol. Soc.* **144** 360–83
- [53] Funk C *et al* 2016 Assessing the contributions of local and East Pacific warming to the 2015 droughts in Ethiopia and southern Africa *Bull. Am. Meteorol. Soc.* **97** S75–S80
- [54] Funk C *et al* 2015 The centennial trends Greater Horn of Africa precipitation dataset *Sci. Data* **2** 150050
- [55] Macleod D and Caminade C 2019 The moderate impact of the 2015 El Niño over East Africa and its representation in seasonal reforecasts *J. Clim.* **32** 7989–8001
- [56] Kilavi M *et al* 2018 Extreme rainfall and flooding over central Kenya including Nairobi City during the long-rains season 2018: causes, predictability, and potential for early warning and actions *Atmosphere* **9** 472
- [57] Rateb A and Hermas E 2020 The 2018 long rainy season in Kenya: hydrological changes and correlated land subsidence *Remote Sens.* **12** 1390
- [58] Wainwright C M, Finney D L, Kilavi M, Black E and Marsham J H 2020 Extreme rainfall in East Africa, October 2019–January 2020 and context under future climate change *Weather* **76** 26–31
- [59] Wainwright C M, Finney D L, Kilavi M, Black E and Marsham J H 2021 Extreme rainfall in East Africa, October 2019–January 2020 and context under future climate change *Weather* **76** 26–31
- [60] Philip S *et al* 2018 Attribution analysis of the Ethiopian drought of 2015 *J. Clim.* **31** 2465–86
- [61] Philippon N, Rouault M, Richard Y and Favre A 2012 The influence of ENSO on winter rainfall in South Africa *Int. J. Climatol.* **32** 2333–47
- [62] Meehl G A, Tebaldi C, Walton G, Easterling D and McDaniel L 2009 Relative increase of record high maximum temperatures compared to record low minimum temperatures in the U.S. *Geophys. Res. Lett.* **36** L23701
- [63] Wolski P, Conradie S, Jack C and Tadross M 2021 Spatio-temporal patterns of rainfall trends and the 2015–2017 drought over the winter rainfall region of South Africa *Int. J. Climatol.* **41** E1303–19
- [64] Sorensen J P R *et al* 2021 The influence of groundwater abstraction on interpreting climate controls and extreme recharge events from well hydrographs in semi-arid South Africa *Hydrogeol. J.* **29** 2773–87
- [65] Ascott M J *et al* 2020 *In Situ* observations and lumped parameter model reconstructions reveal intra-annual to multidecadal variability in groundwater levels in sub-Saharan Africa *Water Resour. Res.* **56** e2020WR028056
- [66] Owor M, Taylor R G, Tindimugaya C and Mwisigwa D 2009 Rainfall intensity and groundwater recharge: empirical evidence from the Upper Nile Basin *Environ. Res. Lett.* **4** 035009
- [67] Cuthbert M O *et al* 2019 Global patterns and dynamics of climate-groundwater interactions *Nat. Clim. Change* **9** 137–41
- [68] Taylor R, Tindimugaya C, Barker J, Macdonald D and Kulabako R 2010 Convergent radial tracing of viral and solute transport in gneiss saprolite *Ground Water* **48** 284–94
- [69] Grey D and Sadoff C W 2007 Sink or Swim? Water security for growth and development *Water Policy* **9** 545–71
- [70] Zeitoun M 2011 The global web of national water security *Global Policy* **2** 286–96
- [71] Howard G, Calow R, Macdonald A and Bartram J 2016 *Annual Review of Environment and Resources* vol 41, ed A Gadgil and T P Gadgil (Palo Alto, CA: ANNUAL REVIEWS) pp 1–465
- [72] Siebert S *et al* 2010 Groundwater use for irrigation—a global inventory *Hydrol. Earth Syst. Sci.* **7** 3977–4021
- [73] Fragaszy S and Closas A 2016 Cultivating the desert: irrigation expansion and groundwater abstraction in northern state, Sudan *Water Altern.* **9** 139–61
- [74] Al-Agha D E, Closas A and Molle F 2015 Survey of groundwater use in the central part of the Nile Delta. *Int. Water Management Institute, Water and Salt Management in the Nile Delta: Report No. 6* pp 3–50
- [75] Tilahun S A *et al* 2020 Establishing irrigation potential of a hillside aquifer in the African highlands *Hydrol. Process.* **34** 1741–53
- [76] Oiro S, Comte J-C, Soulsby C, MacDonald A and Mwakamba C 2020 Depletion of groundwater resources under rapid urbanisation in Africa: recent and future trends in the Nairobi Aquifer System, Kenya *Hydrogeol. J.* **28** 2635–56
- [77] Birhanu B *et al* 2021 Impact of natural and anthropogenic stresses on surface and groundwater supply sources of the upper Awash sub-basin, central Ethiopia *Front. Earth Sci.* **9** 656726

- [78] Healy A *et al* 2020 Domestic groundwater abstraction in Lagos, Nigeria: a disjuncture in the science-policy-practice interface? *Environ. Res. Lett.* **15** 045006
- [79] Edward K, Mekonnen D, Tiruneh S and Ringler C 2019 Sustainable land management and its effects on water security and poverty *Int. Food Policy Res. Inst. Discussion Paper 01811* p 25
- [80] Ebrahim G Y, Villholth K G and Boulos M 2019 Integrated hydrogeological modelling of hard-rock semi-arid terrain: supporting sustainable agricultural groundwater use in Hout catchment, Limpopo Province, South Africa *Hydrogeol. J.* **27** 965–81
- [81] van Steenberg F, Haile A M, Alemehayu T, Alamirew T and Geleta Y 2011 Status and potential of spate irrigation in Ethiopia *Water Resour. Manage.* **25** 1899–913
- [82] Ritchie H, Eisma J A and Parker A 2021 Sand dams as a potential solution to rural water security in drylands: existing research and future opportunities *Front. Water* **3** 651954
- [83] Ojiambo B S, Poreda R J and Lyons W B 2001 Ground water/surface water interactions in Lake Naivasha, Kenya, using delta O-18, delta D, and H-3/He-3 age-dating *Ground Water* **39** 526–33
- [84] Desta H and Lemma B 2017 SWAT based hydrological assessment and characterization of Lake Ziway sub-watersheds, Ethiopia *J. Hydrol.: Reg. Stud.* **13** 122–37
- [85] Molle F, Gaafar I, El-Agha D E and Rap E 2018 The Nile delta's water and salt balances and implications for management *Agric. Water Manage.* **197** 110–21
- [86] Olivier D W and Xu Y X 2019 Making effective use of groundwater to avoid another water supply crisis in Cape Town, South Africa *Hydrogeol. J.* **27** 823–6
- [87] Conrad J, Smit L, Murray K, van Gend-muller J and Seyler H 2019 The Malmesbury group—an aquifer of surprising significance *S. Afr. J. Geol.* **122** 331–42
- [88] MacDonald A M *et al* 2019 Groundwater and resilience to drought in the Ethiopian highlands *Environ. Res. Lett.* **14** 095003
- [89] MacAllister D J, MacDonald A M, Kebede S, Godfrey S and Calow R 2020 Comparative performance of rural water supplies during drought *Nat. Commun.* **11** 1099
- [90] Williams I N and Patricola C M 2018 Diversity of ENSO events unified by convective threshold sea surface temperature: a nonlinear ENSO index *Geophys. Res. Lett.* **45** 9236–44
- [91] Wiedermann M, Siegmund J F, Donges J F and Donner R V 2021 Differential imprints of distinct ENSO flavors in global patterns of very low and high seasonal precipitation *Front. Clim.* **3** 5